

EFFICIENCY CALIBRATION OF A WELL-TYPE HPGe DETECTOR USING EXPERIMENTAL AND MONTE CARLO SIMULATION TECHNIQUES

by

**Ekaterini DALAKA^{1,2*}, Georgios KUBURAS¹,
Konstantinos ELEFThERiADIS¹, and Marios J. ANAGNOSTAKIS²**

¹ Environmental Radioactivity Laboratory, Institute of Nuclear & Radiological Sciences & Technology, Energy & Safety, National Centre for Scientific Research "Demokritos", Agia Paraskevi, Attiki, Greece

² Nuclear Engineering Department, National Technical University of Athens, Athens, Greece

Scientific paper

<https://doi.org/10.2298/NTRP2002121D>

Well-type high-purity germanium detectors are well suited for the analysis of small samples, as they combine high detection efficiency with low background radiation. The well geometry however makes efficiency calibration more difficult than that of ordinary HPGe detectors, due to intense true coincidence and possibly random summing effects. Such a detector has been installed at the Environmental Radioactivity Laboratory of the National Centre for Scientific Research "Demokritos". For the calibration of this detector, experimental and Monte Carlo simulation techniques were applied. To this end, calibration sources were produced from the radionuclides available at the Environmental Radioactivity Laboratory. Starting from the geometrical characteristics of the detector as provided by the manufacturer, using the calibration sources and applying Monte Carlo simulation techniques, the detector was characterized and peak efficiency, as well as total-to-peak calibration curves were produced. The results of the calibration finally obtained by simulation are found to be in good agreement with the respective experimental calibration results.

Key words: gamma ray spectrometry, well-type HPGe detector, Monte Carlo simulation, efficiency calibration

INTRODUCTION

The gamma ray spectrometry with high-purity germanium detectors (HPGe) is very often used in environmental analysis. Environmental samples like aerosol particles collected on filters [1] or thin impaction substrates [2] are often of low activity and therefore it is of great importance to ensure the lowest detection limit possible for the isotopes of interest. Furthermore, some radionuclides of importance for environmental analysis emit low-energy gamma photons in the energy region of 40-100 keV (*e. g.* ²¹⁰Pb, ²⁴¹Am, ²³⁴Th) and have very low emission probabilities.

The detection limit of a radionuclide is improved with increasing detector efficiency and decreasing the background level [3]. To lower the background level of a HPGe crystal, a number of techniques can be used as described in literature [3, 4], such as the proper selection of materials for the shielding and the detector surrounding materials, as well as other considerations with regard to the detection system and the counting

room. With regard to the continuum background produced by the analyzed source sample, detector type, shielding and the source-to-detector geometry play the most important role.

In the case where radionuclides emitting low energy photons need to be determined, the issue of self-absorption inside the sample is of great importance as well [5]. One solution when it comes to environmental samples analysis is the use of well-type detectors instead of coaxial. The reason why a well-type detectors is a preferable choice compared to a coaxial with the same volume is its solid angle of detection. A well-type detector has a solid angle of detection of the order of 4 , much higher than the typical solid angle of standard germanium detectors for cylindrical and Marinelli geometry [6]. As a result, full energy peak efficiency of well-type detectors is 4-5 times higher, compared to coaxial detectors of the same volume when analyzing small sample volumes [3]. Furthermore, in the case of high photon attenuation within the sample (*e. g.* low energy photons, high Z and high-density materials), well-type detectors are again preferred [6].

* Corresponding author; e-mail: edalaka@ipta.demokritos.gr

The increased solid angle and efficiency of well-type detectors however have some disadvantages, since the coincidence summing effects are enhanced, compared to a conventional HPGe [7], introducing significant difficulties in the detector's efficiency calibration and spectrum analysis. Coincidence summing is the result of the simultaneous interaction of two or more photons originating from the decay of the same nucleus with the detector. Coincidence summing effects are of great importance for some radionuclides very often used in detector efficiency calibrations, like ^{60}Co and ^{88}Y . Large NaI(Tl) detectors can be used in anticoincidence and coincidence spectroscopy where the well- or annulus-type crystal surrounds a germanium detector [7].

Well-type detectors are extensively used for the analysis of environmental samples for isotopes emitting low gamma ray energies [3, 5, 6, 8], especially when small amounts of material are available. When using well-type detectors in this kind of analysis, samples are packed into cylindrical holders – much smaller than ordinary sample vials – which are inserted into the detector well, thus increasing efficiency and reducing self-absorption within the sample.

A very common technique for detector efficiency calibration is the use of commercially available mixed radionuclide standards, emitting photons which cover a wide energy range. In the case of a well-type detector calibration however, this may not be the best solution, since these standards include radionuclides like ^{60}Co and ^{88}Y suffering from a true coincidence summing effect, not to mention the random summing effect that may be of major concern for high activity calibration sources. A practical solution is to use a mixture of radionuclides emitting non-coincident gamma-rays that cover the energy region of interest [9] if available. In addition, computation techniques for coincidence summing corrections can be used. These corrections can be applied to the area of the photopeaks suffering from coincidence summing. For a well-type detector where true coincidence effects are more intense the correction calculations need to be performed with greater accuracy than in ordinary HPGe detectors [3].

As a solution to the difficulties of the experimental efficiency calibration of a well-type detector, Monte Carlo simulation techniques can be also used [3, 6, 8]. According to [10-12] the use of Monte Carlo codes in order to produce full energy efficiency curves can result in an accuracy of 2-3 % in most cases and an accuracy of 5-10 % when it comes to complex geometries and isotopes emitting low energy photons.

The most important step when using Monte Carlo simulation techniques in order to calibrate a detector is the formation of the file that describes the simulated geometry, as it can be the main source of the efficiency's inaccuracy. However, some of the detector geometrical characteristics needed for the simulation

are in most cases, either not provided by the manufacturer, or presented with high uncertainty. Furthermore, information on the detector's dead layers is in most cases inadequate or even missing. The dead layers are inactive regions within the detector crystal, and therefore, when a photon interacts within this region no signal is recorded in the energy spectrum. The thickness and shape of the dead layers differ from crystal to crystal, as well as within the same crystal, and their dimensions can only be estimated. Furthermore, they depend on the detector's high voltage and may change with time, especially after a warmed-up/cooled-down cycle [8].

The aim of this work is the efficiency calibration of a well-type germanium detector, using both Monte Carlo simulation and experimental techniques. The use of Monte Carlo techniques as an efficiency calibration tool has been reported in other studies [3, 5, 6, 8, 13-15]. In this work, for the purpose of calibration, custom-made calibration sources, based on materials available at the Environmental Radioactivity Laboratory of the NCSR – “Demokritos” (ERL) were produced. The procedure that was followed for source production and the detector's calibration is analyzed in detail in the paragraphs to follow.

MATERIALS AND METHODS

Experimental set-up

The detector used in this work is a Canberra well-type HPGe, installed at the ERL with relative efficiency 20.6 %, FWHM = 2.2 keV at 1.33 MeV and FWHM = 1.4 keV at 122 keV. The detector has a crystal height of 57.0 mm, diameter of 54.4 mm and a well depth and diameter of 35.5 mm and 22.5 mm respectively. The crystal is mounted inside a 1.5 mm thick aluminum endcap. The detector is shielded with 10.6 cm lead covered inside with 2 mm electrolytic copper. For spectrum collection and analysis Genie 2000 data acquisition and analysis software is used.

Efficiency calibration sources

For the experimental efficiency calibration and detector characterization, calibration sources based on materials available at the ERL were produced. The option of preparing a calibration source from the mixed radionuclide standard usually used for calibrations at the ERL (CBSS 2), was rejected due to the significant coincidence summing of some of the radionuclides it contains (^{60}Co , ^{88}Y). For the calibration, a total of six calibration samples (sources) were produced, fig. 1, two with a cellulose filter as a matrix, one based on an ALMERA intercomparison sample, one using K_2CO_3 powder and two out of soil-dust. The sources contain



Figure 1. Volume sources produced for the calibration of the well-type detector

radionuclides carefully selected in order to cover in the best possible way the energy region of interest (70-1800 keV), using as matrices materials that simulate the actual samples usually analyzed at the ERL. The procedure that was followed for source production is analyzed in detail in the following paragraphs.

Volume sources using cellulose filters as a matrix

Since one of the major activities at the ERL is the analysis of air filters, it was considered necessary to prepare calibration sources with the same matrix as the cellulose filters used. For this purpose the following radionuclides available at the ERL were used:

- liquid solution of ^{243}Am (1.865 Bqml^{-1} , standard unc 7.4 %) with a half-life of 7370 years, emitting photons with energies at 43.5 keV and 74.66 keV.

- liquid solution of ^{226}Ra (10.0 Bqml^{-1} , standard unc 0.8 %) with a half-life of 1600 years, emitting photons at 186.2 keV.

The two sources were produced by adding one ml of each solution to Whatman cellulose filters, using a calibrated micropipette of 20 μl (standard unc 0.5 %). This pipette was selected in order to have the best possible distribution of the radioactive solution on the filters and a source as homogenous as possible was produced. Once the filter dried out, it was folded and inserted into a glass vial, having the appropriate geometry for the detector well.

The ^{243}Am source was analyzed twice with the well-type detector for 86400 seconds in order to verify the repeatability of the measurement. The results are presented in tab. 1. For the repeatability verification a U-test was performed, showing that there is no statistical difference between the two measurements. In tab. 1 the uncertainty given is the standard uncertainty (Type A) of the measurement that was used for the repeatability verification with the U-test.

As seen in tab. 1, for the 43.5 keV photons the difference between the two measurements – though not statistically significant – is relatively high. For this reason the 43.5 keV photons were not taken into consideration for the efficiency calibration of the detector.

The ^{226}Ra source was analyzed twice with the well-type detector for 86400 seconds, in order to verify the repeatability of the measurement. The ^{226}Ra emits gamma rays, with the most intense at 186.2 keV and produces a series of short-lived decay products which emit several photons as well. Many of these photons suffer from true coincidence summing, which is intense because of the detector's geometry [8, 13]. Among the photons emitted by ^{226}Ra and its' short lived decay products in equilibrium, the most suitable to be used for the well-type detector's calibration are: 186.2 keV (^{226}Ra), 295.2 keV (^{214}Pb), and 351.9 keV (^{214}Pb). The analysis results are presented in tab. 2. The measurements were conducted six months after the sample's production and shielding, so a radioactive equilibrium between ^{226}Ra and ^{214}Pb was assumed. In tab. 2 the uncertainty given is the standard uncertainty

Table 1. Results of ^{243}Am source analysis

Nuclide	E [keV]	February 2 nd 2018		June 6 th 2018		Deviation [%]	U-test
		Eff counted)	Eff counted)		
^{243}Am	43.5	0.387	5	0.431	5	-11	0.598
	74.7	0.557	5	0.566	5	-2	0.121

Table 2. Results of ^{226}Ra and ^{214}Pb source analysis

Nuclide	E [keV]	February 8 nd 2018		June 4 th 2018		Deviation [%]	U-test
		Eff counted)	Eff counted)		
^{226}Ra	186.2	0.353	5	0.368	5	-4	0.204
	^{214}Pb	295.2	0.167	5	0.164	5	1
351.9		0.133	5	0.130	5	2	0.043

(Type A) of the measurement that was used for the repeatability verification with the *U*-test.

As seen in tab. 2 the deviation and the *U*-test performed revealed that these two analyses are statistically the same confirming repeatability of the measurement.

Volume source produced using ALMERA intercomparison samples

For the detector's calibration a source containing ^{137}Cs was also prepared. ^{137}Cs emits gamma rays at 661.66 keV with high intensity and is a very important radionuclide when it comes to environmental analysis. For the calibration source fabrication, a milk powder sample spiked with ^{137}Cs was used. This sample was distributed under the ALMERA Proficiency Test IAEA-TEL-2017-04 and at the reference date (October 23, 2017) contained $98.6 \pm 5 \text{ Bqkg}^{-1} \text{ }^{137}\text{Cs}$ (dry). From the original sample a total of 2.8096 g were used for the production of the calibration source inside a glass vial. The sample moisture was estimated at 3.7%. In tab. 3 the analysis results of the ^{137}Cs sample are presented. The ^{137}Cs also emits a series of X-rays at the energies $\sim 32 \text{ keV}$ and $\sim 36 \text{ keV}$. These photopeaks were not used for calibration since they were not well resolved and there was no interest in calibration in this low energy region. Besides, for such low energy photons, self-attenuation correction issues within the sample should probably be taken into consideration.

Volume source produced using chemical compounds available at the ERL

The ^{40}K is a natural radionuclide with a half-life of $1.248 \cdot 10^9$ years emitting gamma ray rays at 1460.8 keV, which makes it suitable for efficiency calibration in the high energy region. For the production of a ^{40}K source, a high purity (99%) K_2CO_3 powder available at the ERL was used. This material is highly hygroscopic, so the water content of the material had to be removed. In total 3.936 g (standard unc 6.7%) of dried K_2CO_3 powder were used. The ^{40}K activity of the source was calculated at 70.93 Bq.

Again, the source was analyzed twice and the analyses results are presented in tab. 4. The uncer-

Table 3. Results of ^{137}Cs source analysis. The results are accompanied by their combined standard uncertainty

Nuclide	E [keV]	July 27 th 2018	
		Eff counted)
^{137}Cs	661.66	0.088	7

Table 4. Results of the ^{40}K calibration source analyses

Nuclide	E [keV]	May 23 th 2018		June 18 th 2018		Deviation [%]	<i>U</i> -test
		Eff counted)	Eff counted)		
^{40}K	1460.8	0.0351	5	0.0349	5	0.6	0.003

tainty given in tab. 4 is the standard uncertainty (Type A) of the measurement that was used for the repeatability verification with the *U*-test.

As seen in tab. 4 the deviation and the *U*-test performed revealed that these two analyses are statistically the same, confirming repeatability of the measurement.

Volume source produced using environmental samples

One main isotope of interest when it comes to aerosol's analysis in terms of gamma spectrometry is ^7Be (a natural isotope of cosmogenic origin, with a half-life of 53.22 days, emitting photons at 477.6 keV). It was therefore considered important to have an estimation of detector efficiency at the ^7Be photon energy of 477.6 keV. To this end – and since no ^7Be source was available at the ERL – the possibility of preparing a calibration source using fine dust of freshly sampled surface soil containing ^7Be was examined. This sample was prepared at the Nuclear Engineering Department of the National Technical University of Athens (NED-NTUA). For this purpose after a rain event, when ^7Be was scavenged and deposited on the ground surface [16-18], an ample quantity of surface soil was collected. The sample was air dried, sieved below 63 μm , homogenized and measured at NED-NTUA, using high resolution high efficiency gamma spectroscopy techniques. Its activity was estimated at 40 Bqkg^{-1} (combined standard unc 7.6%). Then, a sufficient quantity of this material was used to prepare a sample in a glass vial of the same type used for the production of the other calibration sources. The sample was analyzed on the well-type detector for 241015 seconds, tab. 5. As for the second calibration source that was produced out of the surface soil, it was decided not to be analyzed, as it was prepared only as a second identical sample, that was to be used in case of a faulty analysis.

MONTE CARLO SIMULATION

In addition to the experimental work, Monte Carlo simulation techniques were applied in order to verify and extend the experimental calibration. Monte Carlo simulation codes have been developed and used

Table 5. Results of ^7Be source analysis. The results are accompanied by their combined standard uncertainty

Nuclide	E [keV]	July 27 th 2018	
		Eff counted)
^{137}Cs	661.66	0.088	7

as an alternative way to study the interactions between radiation and matter. For this study the Monte Carlo code PENELOPE 2011 and its user code PENMAIN were used [19].

Initial detector simulation

For modeling the detector geometry, the geometrical characteristics provided by the detector's manufacturer were used as a base and cylindrical symmetry was assumed for all components of the sample-detector geometry. As presented in the detector technical sheets, the crystal is surrounded by a holder made of copper and an insulator made of Teflon. In order to speed-up the simulation process, an effort was made to simplify the detector geometry. To this end the effect of including or not including the copper made holder and the Teflon insulator in the simulation was investigated. Figure 2 shows the geometry files that were produced, with and without taking into account the extra materials surrounding the crystal, as visualized using the GEVIEW2D.

One of the detector's characteristics that needed further investigation was the dead layer thickness. The dead layer is the result of the addition of *p*- or *n*-type impurities to the Ge crystal surface in order to produce the PIN junction of the detector. For well-type detectors, a

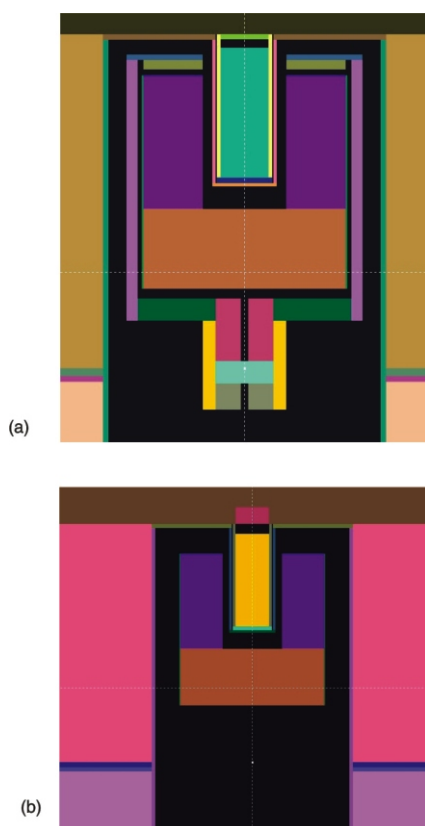


Figure 2. Two different versions of the geometry file: (a) detailed geometry including the holder and teflon insulator; and (b) simplified geometry without the copper holder and teflon insulator

few weeks after the detector fabrication production the dead layer thickness ranges between 0.3-0.4 mm. However, some months later it may reach ~0.8 mm and in some cases even 2 mm [3]. In order to keep dead layer thickness at a minimum and constant thickness with time, the crystal was cooled down as soon as it was installed at the ERL and is kept cooled ever since. According to the detector specifications and the literature available in this field, for these testing simulations the front and peripheral dead layer was set at 0.5 mm and the well dead layer was set at $3 \cdot 10^{-4}$ mm. Table 6 presents the efficiency simulation results for the two geometries presented in fig. 2, and a comparison between them.

As seen in tab. 6 the efficiencies calculated using PENELOPE 2011 for the detailed and the simplified geometries are statistically the same. So, it does not make any difference whether the simple or the detailed geometry are used for the simulations. Furthermore, simulation speed is not so much affected by the geometry simplification. For this study it was finally decided to use the detailed geometry since the effect of using the simpler geometry on the simulation speed was considered negligible. It should be also mentioned that while the full energy peak efficiency is the same for both geometries, the total efficiency is not, since the materials surrounding the detector may significantly affect the scattered photons which reach the detector.

Simulation model

For the determination of the detector's efficiency using simulation techniques it is necessary to have geometrical information for the source and the detector with the highest accuracy possible. While for the source this information is relatively easy to obtain, this is not always the case for the detector, as it has already been explained. In this study, in order to obtain a good set of geometrical characteristics to be used as an input for the simulation, an iterative method was applied as described in [15]. Starting from the information provided by the manufacturer, a series of photon energies were simulated and then the efficiency for the corresponding energies was calculated and compared with the available experimental efficiencies. Then, simulations were repeated with the geometry file slightly modified in order to make simulation efficiency results converge with the experimental ones. This process was repeated until acceptable convergence was reached, given a predefined convergence criterion [15]. The parameters modified between iterations were the most uncertain – like dead layer thickness – and those having the greater effect on detector efficiency. At the end of the iteration process, a set of detector geometrical characteristics was adopted. This set of data lead to the best efficiency response of the detector that was tested. It should be noted however that the final source-detector geometry set that was determined fol-

Table 6. Efficiency simulation results for the detailed and simplified geometry

Nuclide	E [keV]	Efficiency simulated (simple geometry)	$\sigma\%$ (1)	Simulation speed (showers per second)	Simulation time [s]	Simulated primary showers
²⁴³ Am	74.66	0.550	0.01	$5.24 \cdot 10^4$	$2.99 \cdot 10^3$	$1.57 \cdot 10^8$
²²⁶ Ra	186.21	0.386	0.02	$1.33 \cdot 10^4$	$2.99 \cdot 10^3$	$3.99 \cdot 10^7$
²¹⁴ Pb	295.22	0.230	0.05	$5.02 \cdot 10^3$	$2.99 \cdot 10^3$	$1.50 \cdot 10^7$
²¹⁴ Pb	351.93	0.188	0.06	$3.75 \cdot 10^3$	$3.00 \cdot 10^3$	$1.12 \cdot 10^7$
⁷ Be	477.60	0.134	0.11	$2.45 \cdot 10^3$	$2.40 \cdot 10^3$	$5.86 \cdot 10^6$
⁴⁰ K	1460.82	0.045	0.30	$8.07 \cdot 10^2$	$2.99 \cdot 10^3$	$2.41 \cdot 10^6$
Nuclide	E [keV]	Efficiency simulated (complex geometry)	$\sigma\%$ (1)	Simulation speed (showers per)	Simulation time [s]	Simulated primary showers
²⁴³ Am	74.66	0.550	0.01	$4.18 \cdot 10^4$	$3.00 \cdot 10^3$	$1.25 \cdot 10^8$
²²⁶ Ra	186.21	0.386	0.02	$1.22 \cdot 10^4$	$2.98 \cdot 10^3$	$3.64 \cdot 10^7$
²¹⁴ Pb	295.22	0.230	0.05	$5.03 \cdot 10^3$	$2.98 \cdot 10^3$	$1.50 \cdot 10^7$
²¹⁴ Pb	351.93	0.188	0.06	$3.89 \cdot 10^3$	$3.00 \cdot 10^3$	$1.17 \cdot 10^7$
⁷ Be	477.60	0.134	0.10	$2.47 \cdot 10^3$	$2.39 \cdot 10^3$	$5.91 \cdot 10^6$
⁴⁰ K	1460.82	0.045	0.33	$8.33 \cdot 10^2$	$3.00 \cdot 10^3$	$2.50 \cdot 10^6$
Nuclide	E [keV]	U -test				
²⁴³ Am	74.66	0.0002				
²²⁶ Ra	186.21	0.0001				
²¹⁴ Pb	295.22	0.0000				
²¹⁴ Pb	351.93	0.0000				
⁷ Be	477.60	0.0000				
⁴⁰ K	1460.82	0.0001				

lowing this procedure, is the one that best describes the simulated geometry and does not necessarily correspond to the actual source-detector geometry.

Another issue that had to be taken into consideration was the calibration source matrices. Since the information available for each material was only a

Table 7. Initial and final dimension set based on the detector's certificate and the Monte Carlo simulations

	Initial dimension set	Final dimension set
Diameter	54.4 mm	54.4 mm
Length	57.0 mm	57.0 mm
Distance from window	10.0 mm	10.0 mm
Crystal hole depth	35.5 mm	35.5 mm
Cristal hole diameter	22.5 mm	22.5 mm
End cap-crystal distance	10.9 mm	10.9 mm
End-cap thickness	1.5 mm	1.5 mm
Front dead layer	0.5 mm	0.15 mm
Internal dead layer	0.3 mm	0.15 mm
Dead layer on the bottom of the well	0.3 mm	0.15 mm
Internal well-dead layer	0.5 mm	

general description like soil, dry milk *etc.* some assumptions had to be made for the simulation. The sources made of cellulose filters (²⁴³Am and ²²⁶Ra) were simulated as homogenous cylinders made of cellulose. The milk-powder source of ¹³⁷Cs was simulated as lactose (C₁₂H₂₂O₁₁) with a density of 0.585 gcm⁻³. The ⁴⁰K source was simulated as K₂CO₃ with a density of 0.759 gcm⁻³. For the ⁷Be source things were a bit more complicated. This source was actually sandy soil collected at the NTUA Campus. Therefore it was simulated as SiO₂, with a density of 1.236 gcm⁻¹. In each case the sources were assumed to be homogeneous. It should be mentioned that due to the small size of the calibration sources, the effect of the source matrix on the self-absorption of the photons inside the sources is minimized – at least for the energies tested – therefore a unique calibration curve was obtained for the glass vial geometry even though different materials were used for the calibration.

Table 7 summarizes the geometrical characteristics initially used and those finally adopted from the iteration process.

Table 8. Experimental and simulation full energy peak efficiency of the well-type detector

Nuclide	E [keV]	Experimental efficiency	$\sigma\%$ (1)	Simulation efficiency	$\sigma\%$ (1)	Deviation [%]	U -test
²⁴³ Am	74.66	0.566	9	0.522	0.01	8	0.485
²²⁶ Ra	186.21	0.368	5	0.350	0.03	5	0.363
²¹⁴ Pb	295.22	0.164	5	0.202	0.06	-23	0.748
²¹⁴ Pb	351.93	0.130	5	0.163	0.08	-25	0.661
⁷ Be	477.60	0.111	12	0.115	0.10	-3	0.030
¹³⁷ Cs	661.66	0.088	7	0.084	0.16	5	0.058
⁴⁰ K	1460.82	0.035	8	0.037	0.36	-6	0.028

As seen in tab. 7 the thickness of the dead layers as finally adopted is rather large, compared to the values provided by the manufacturer, yet consistent with values given in literature [3, 8].

In an effort to have more experimental points for the calibration, the ^{214}Pb photons at 295.22 and 351.99 keV were also simulated, under the assumption of radioactive equilibrium with ^{226}Ra . This assumption was considered valid, as the vial containing the ^{226}Ra source was air shielded using an epoxy resin. This technique has been used for years at the NED-NTUA and has been proven sufficient for shielding sources containing ^{226}Ra .

In tab. 8 both the experimental efficiencies and the ones determined by the Monte Carlo simulation for the detector model finally adopted are presented, along with their combined standard uncertainties, and their deviations. The same table presents the results of the U -test that was performed to check their statistical difference.

As can be observed in tab. 8, there are large differences between experimental and simulation results for the 295.22 and 351.99 keV photons, though not statistically significant. A possible explanation for this might be the leakage from the source vial – though it is considered air-shielded – which does not allow for radioactive equilibrium between ^{226}Ra , ^{222}Rn and their short lived progenies to be established. Another possible explanation is the inhomogeneity of the source that was produced with the folded air filter inside the vial. A source not homogeneous or not completely filled with the paper filter results in an inhomogeneous distribution of radon and its short lived progenies in the vial, and thus in an erroneous efficiency. For this reason these two experimental points were rejected from the detector's calibration.

With regard to the rest of the photon energies used, as it is observed in tab. 8, it is clear that with the sources used it has proven difficult to reduce the difference between experimental and simulation efficiencies below ~8 % (for the energy 74.66 keV). This 8 % should be considered as the Type B expanded uncertainty ($k = 3$) of the efficiency values obtained from the calibration curve that is produced from simulation data, given that the respective random uncertainties introduced by the simulation were considered as negligible as they are much lower.

EFFICIENCY CALIBRATION CURVES

With the geometrical characteristics of the detector determined, a series of simulations for various photon energies were performed to adequately cover the energy range of interest 70-1800 keV. Full energy peak efficiency, total efficiency, as well as the ratio of the total-efficiency to the peak-efficiency (total-to-peak ratio – TTP) was calculated for all photon

energies that were simulated. The TTP ratio is necessary for true coincidence summing corrections. The results of these calculations are presented in tab. 9.

In order to improve the efficiency calibration curve several photon energies – not only the ones for which experimental points existed – were also simulated. Figure 3 shows the experimental and simulation efficiency points, as well as the efficiency curve produced from the simulation results. The efficiency fitting function is a 7th degree polynomial, in the form of

$$y = 3.6 \cdot 10^3 + 4.4 \cdot 10^3 \ln x + 2.3 \cdot 10^3 (\ln x)^2 + 6.8 \cdot 10^2 (\ln x)^3 + 1.2 \cdot 10^2 (\ln x)^4 + 1.2 \cdot 10 (\ln x)^5 + 0.7 \cdot 10^1 (\ln x)^6 + 0.2 \cdot 10^1 (\ln x)^7$$

with a r -square of 0.99982.

Figure 4 shows the total efficiency curve and fig. 5 shows the TTP efficiency curve of the well-type detector as determined via the simulation. The efficiency fitting functions are an 8th degree polynomial, with r -squares of 0.99982 (for the total efficiency curve in fig. 4 and 0.99987 (for the TTP efficiency curve in fig. 5).

Table 9. Total efficiency and TTP ratio for the well-type detector

Nuclide	E [keV]	Total efficiency	$\sigma\%$ (1)	TTP	$\sigma\%$ (1)
^{243}Am	74.66	0.67	0.01	1.28	0.01
^{226}Ra	186.21	0.56	0.02	1.60	0.03
^{214}Pb	295.22	0.47	0.04	2.31	0.07
^{214}Pb	351.93	0.44	0.05	2.68	0.09
^7Be	477.60	0.40	0.06	3.44	0.12
^{137}Cs	661.66	0.35	0.04	4.21	0.17
^{40}K	1460.82	0.27	0.10	7.20	0.39

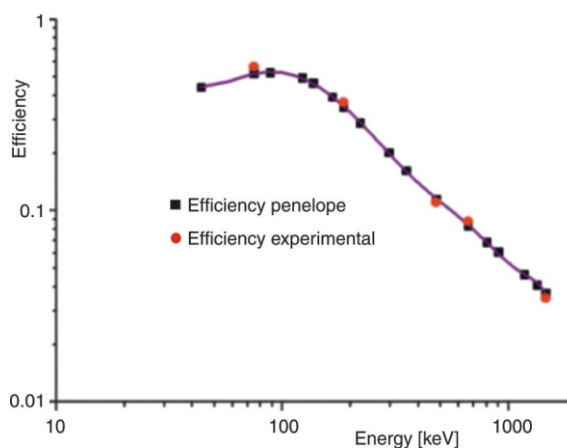


Figure 3. Experimental and simulated efficiency for the well-type detector. The efficiency calibration curve is obtained using the simulation results

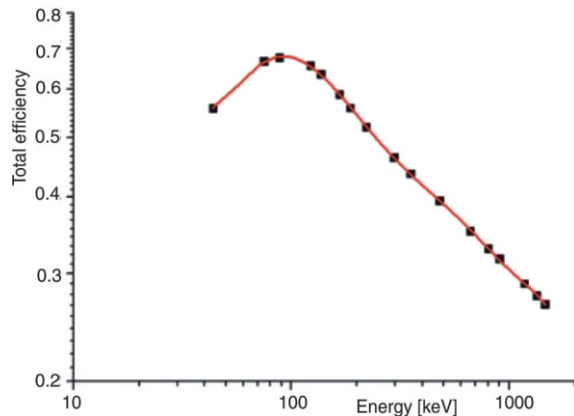


Figure 4. Total efficiency curve using the Monte Carlo code PENELOPE 2011. This graph is on a logarithmic scale

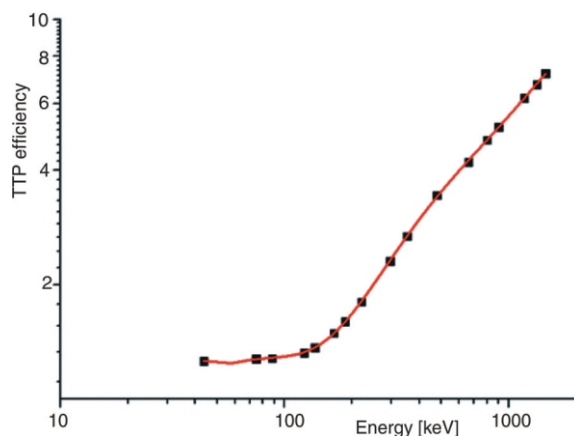


Figure 5. The TTP efficiency using the Monte Carlo simulation

CONCLUSIONS

The efficiency response of a well-type detector, for the analysis of air filters folded in standard glass vial geometry was determined using Monte Carlo simulation techniques. For the detector characterization an iterative method based on the comparison of experimental and Monte Carlo simulation obtained efficiencies was applied. To this end custom-made volume sources were produced and used. The deviations between the experimental efficiencies and the simulated ones were below 8 %, which was considered as low, compared with the Type A uncertainties introduced during the measurement of air filters. This 8% should be considered as Type B uncertainty of the detector calibration and should be incorporated in uncertainty budget calculations of the activities determined in future analyses of air-filters. The full energy peak efficiency as well as the total efficiency and the TTP ratio correlations with energy were determined and plotted for the well-type detector.

ACKNOWLEDGMENT

We acknowledge the support of this work by the project “NCSR – INRASTES research activities in the framework of the national RIS3.” (MIS 5002559) which is implemented under the “Action for the Strategic Development on the Research and Technological Sector”, funded by the Operational Program “Competitiveness, Entrepreneurship and Innovation” (NSRF 2014-2020) and co-financed by Greece and the European Union (European Regional Development Fund).

AUTHORS CONTRIBUTIONS

The lead author E. Dalaka conducted the Monte Carlo simulations, experimental work, analyzed the experimental data and wrote the paper. All the other authors made an equal contribution in supporting and advising A. Dalaka in all aspects of this research and reviewing the paper.

REFERENCES

- [1] Kritidis, P., et al., Radioactive Pollution in Athens, Greece due to the Fukushima Nuclear Accident, *Journal of Environmental Radioactivity*, 114 (2011), Dec., pp. 100-104
- [2] Masson, O., et al., Size Distributions of Airborne Radionuclides from the Fukushima Nuclear Accident at several Places in Europe, *Environmental Science and Technology*, 47 (2013), 19, pp. 10995-11003
- [3] Laborie, J. M., et al., Monte Carlo Calculation of the Efficiency Response of a Low-Background Well-Type HPGe Detector, *Nuclear Instruments and Methods in Physics Research, A* 479 (2002), pp. 618-630
- [4] Heusser, G., Low-Radioactivity Background Techniques, *Annu. Rev. Nucl., Part. Sci.*, 45 (1995), pp. 543-90
- [5] Appleby, P. G., et al., Self-Absorption Corrections for Well-Type Germanium Detectors, *Nuclear Instruments and Methods in Physics Research, B* 71 (1992), pp. 228-233
- [6] Sima, O., Arnold, D., Self-Attenuation and Coincidence-Summing Corrections Calculated by Monte Carlo Simulations for Gamma-Spectrometric Measurements with Well-Type Germanium Detectors, *Applied Radiation and Isotopes*, 47 (1996), 9/10, pp. 889-893
- [7] Hansman, J., Design and Construction of a Shield for the 9"x9" NaI(Tl) Well-Type Detector, *Nucl Technol Radiat*, 29 (2014), 2, pp. 165-169
- [8] Laborie, J. M., et al., Monte Carlo Calculation of the Efficiency Calibration Curve and Coincidence-Summing Corrections in Low-Level Gamma-Ray Spectrometry Using Well-Type HPGe Detectors, *Applied Radiation and Isotopes*, 53 (2000), 1-2, pp. 57-62
- [9] Sanderson, C. G., Decker, K. M., A Mixed Gamma-Ray Standard for Calibrating Germanium Well Detectors, *Radioactivity and Radiochem.*, 4 (1993), 2, p. 36
- [10] Sima, O., Applications of Monte Carlo Calculations to Gamma-Spectrometric Measurements of Environmental Samples, *Applied Radiation and Isotopes*, 47 (1996), 9/10, pp. 919-923

- [11] Decombaz, M., et al., Coincidence-Summing Corrections for Extended Sources in Gamma-Ray Spectrometry Using Monte Carlo Simulation, *Nucl. Instr. Meth., A*, 312 (1992), 152
- [12] Bronson, F. L., Wang, L., Canberra, Validation of the MCNP Monte Carlo Code for Germanium Detector Gamma Efficiency Calibrations, *Proceedings, Waste Management'96*, 1996, Tucson, Ariz, USA
- [13] Reyss, J. L., et al., Large, Low Background Well-Type Detectors for Measurements of Environmental Radioactivity, *Nuclear Instruments and Methods in Physics Research, A* 357 (1995), pp. 391-397
- [14] Sima, O., Accurate Calculation of Total Efficiency of Ge Well-Type Detectors Suitable for Efficiency Calibration Using Common Standard Sources, *Nuclear Instruments and Methods in Physics Research, A* 450 (2000), pp. 98-108
- [15] Agrafiotis, K., et al., Calibration of an In-Situ BEGe Detector Using Semi-Empirical and Monte Carlo techniques, *Applied Radiation and Isotopes*, 69 (2011), 8, pp. 1151-1155
- [16] Monaghan, M. C., Lead-210 in Surface and Soils from California: Implications for the Behavior of Trace Constituents in the Planetary Layer, *Journal of Geophysical Research*, 94 (1989), D5, pp. 6449-6456
- [17] Likuku, A. S., Factors Influencing Ambient Concentrations of ^{210}Pb and ^7Be Over the City of Edinburgh, *Journal of Environmental Radioactivity*, 87 (2006), 3, pp. 289-304
- [18] Duenas, C., et al., ^7Be to ^{210}Pb Concentration Ratio in Ground Level air in Malaga (36.7 °N, 4.5°W), *Atmospheric Research*, 92 (2009), 1, pp. 49-57
- [19] Baro, J., et al., PENELOPE: An Algorithm for Monte Carlo Simulation of the Penetration and Energy Loss of Electrons and Positrons in Matter, *Nuclear Instruments and Methods in Physics Research Section B: Beam Interactions with Materials and Atoms*, 100 (1995), 1, pp. 31-46

Received on July 15, 2020

Accepted on September 9, 2020

**Катерина ДАЛАКА, Георгиос КУБУРАС,
Константинос ЕЛЕФТЕРИАДИС, Мариос Ј. АНАГНОСТАКИС**

**КАЛИБРАЦИЈА ЕФИКАСНОСТИ ГЕРМАНИЈУМСКОГ ДЕТЕКТОРА
ВИСОКЕ ЧИСТОЋЕ И ЈАМСКОГ ТИПА, ЕКСПЕРИМЕНТАЛНИМ ПОСТУПЦИМА
И МОНТЕ КАРЛО СИМУЛАЦИОНИМ ТЕХНИКАМА**

Детектори јамског типа са германијумом високе чистоће веома су погодни за анализу малих узорака, јер комбинују високу ефикасност детекције са малим позадинским зрачењем. Међутим, геометрија јаме отежава калибрацију ефикасности у поређењу са обичним детекторима са германијумом високе чистоће, због јаке праве коинциденције и кумулације могућих случајних ефеката. Такав детектор је инсталисан у Лабораторији за радиоактивност животне средине Националног центра за научна истраживања "Демокритос". За калибрацију овог детектора примењене су експерименталне и Монте Карло технике симулације. У ту сврху произведени су извори за калибрацију од радионуклида доступних у Лабораторији. Полазећи од геометријских карактеристика детектора које је обезбедио произвођач, користећи изворе калибрације и примењујући Монте Карло симулационе технике, детектор је окарактерисан и произведене су калибрационе криве ефикасности у пику, као и односа тоталне ефикасности и ефикасности у пику. Утврђено је да се резултати калибрације коначно добијени симулацијом добро слажу са одговарајућим резултатима експерименталне калибрације.

Кључне речи: џама сѝекѝрометѝрија, деѝекѝор ѝиѝија јаме, ѝерманијум високе чистоће
Монѝе Карло симулација, калибрација ефикасности